Role of PCET in the Redox Interconversion between Benzoquinone and Hydroquinone.

ARTICLE *in* JOURNAL OF THE AMERICAN CHEMICAL SOCIETY · NOVEMBER 2012

Impact Factor: 12.11 · DOI: 10.1021/ja308700t · Source: PubMed

6 AUTHORS, INCLUDING:

Na Song
University of North Carolina at Chapel Hill
16 PUBLICATIONS **155** CITATIONS
SEE PROFILE

Ming-Tian Zhang
Tsinghua University
21 PUBLICATIONS **397** CITATIONS
SEE PROFILE

JACS
JOURNAL OF THE AMERICAN CHEMICAL SOCIETY
Communication
pubs.acs.org/JACS

Role of Proton-Coupled Electron Transfer in the Redox Interconversion between Benzoquinone and Hydroquinone

Na Song, Christopher J. Gagliardi, Robert A. Binstead, Ming-Tian Zhang, Holden Thorp, and Thomas J. Meyer*

Department of Chemistry, University of North Carolina at Chapel Hill, Chapel Hill, North Carolina 27599-3290, United States

Supporting Information

ABSTRACT: Benzoquinone/hydroquinone redox interconversion by the reversible $Os(dmb)_3^{3+/2+}$ couple over an extended pH range with added acids and bases has revealed the existence of seven discrete pathways. Application of spectrophotometric monitoring with stopped-flow mixing has been used to explore the role of PCET. The results have revealed a role for phosphoric acid and acetate as proton donor and acceptor in the concerted electron−proton transfer reduction of benzoquinone and oxidation of hydroquinone, respectively.

Derivatives of benzoquinone/hydroquinone (Q/H_2Q) play essential roles in biology.[1] An important example appears in photosynthesis, in the reduction of plastoquinone (Q_B) to the mobile redox carrier plastoquinol (H_2Q_B), which is transported through the thylakoid membrane to cytochrome b_6f, where it is oxidized to Q_B with proton release to the lumen.[2]

Interconversion between Q and H_2Q in photosystem II (PSII) and amino acid redox mediators in biology utilize proton-coupled electron transfer (PCET) in transferring redox equivalents with the transfer of both electrons and protons.[1a] In tyrosine and cysteine oxidation, concerted electron−proton transfer (EPT) pathways are utilized to avoid high-energy protonated radical intermediates.[3,4] In these reactions, pendant bases or solvent molecules enable EPT by acting as H^+ acceptors avoiding high-energy intermediates like $TyrOH^{\bullet+}$.[3] For tyrosine oxidation, $E^\circ \approx 1.5$ V (vs NHE) for $1e^-$ oxidation to $TyrOH^{\bullet+}$, compared to $E^\circ \approx 1.0$ V for oxidation of the tyrosine−histidine acid−base pair in PSII, TyrOH---His → $TyrO^{\bullet}$---$^+$H-His.[2a−c]

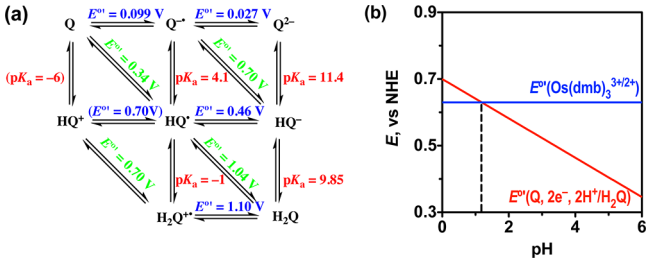

Figure 1. (a) $E^{\circ\prime}$(vs NHE)−pK_a diagram for the Q/H_2Q couple. Diagonal lines give potentials vs NHE for $1H^+/1e^-$ PCET couples at pH 0 in water. pK_a for HQ^+ was obtained in the present work. (b) Calculated $E^{\circ\prime}$−pH diagram for Q/H_2Q (red) and $Os(dmb)_3^{3+/2+}$ (blue) couples.

Amino acid oxidation is irreversible, but the Q/H_2Q couple is reversible, providing an opportunity for mechanistic investigation in "both directions". There is an extensive literature on Q/H_2Q redox interconversion,[5] but very little is known about the role of acid- and base-assisted PCET pathways.

We report here mechanistic details of the redox interconversion between Q and H_2Q as a function of pH by the couple $Os(dmb)_3^{3+/2+}$ (dmb = 4,4′-dimethyl-2,2′-bipyridine). Remarkably, our results provide evidence for seven distinct pathways for this interconversion, including an important role for concerted EPT that may be of relevance in biological Q/H_2Q reactions.

Results of extensive electrochemical measurements on Q/H_2Q interconversion are available,[6] but interpretation is typically complicated by adsorption and mass-transfer effects. Following Laviron, a potential−pK_a diagram for the Q/H_2Q couple under standard conditions is shown in Figure 1a.[7] From the diagram the $1e^-$ semiquinone intermediate, $HQ^{\bullet}$, is highly unstable toward disproportionation, $2HQ^{\bullet} \rightarrow H_2Q + Q$, with $\Delta G^\circ = -0.7$ eV.[8]

The implied importance of PCET and concerted EPT[2a,b,9] in Q/H_2Q reactivity is apparent from the $E^{\circ\prime}$−pK_a diagram. For PCET reduction of Q to $HQ^{\bullet}$, $E^{\circ\prime}(Q/HQ^{\bullet}) = 0.34$ V (vs NHE). In a mechanism involving initial proton transfer, $Q + H^+ \rightleftharpoons HQ^+$, followed by electron transfer, $HQ^+ + e^- \rightarrow HQ^{\bullet}$ (PT-ET), protonation is unfavorable, with $pK_a(HQ^+) \approx -6$ and $\Delta G^{\circ\prime} = -0.059(pH+6) = 0.35$ eV at pH 0. HQ^+ is an enhanced oxidant with $E^{\circ\prime}(HQ^+/HQ^{\bullet}) = 0.70$ V (vs NHE). For electron transfer followed by proton transfer (ET-PT), $E^{\circ\prime}(Q/Q^{-\bullet}) = 0.099$ V for the initial electron transfer, with $\Delta G^{\circ\prime} = -0.24$ eV for protonation of $Q^{-\bullet}$ at pH 0.

As shown in Figure 1b, $E^{\circ\prime} = 0.63$ V (vs NHE) for the $Os(dmb)_3^{3+/2+}$ couple, and it is pH-independent. The Os complexes are substitutionally inert and have minimal barriers to electron transfer.[10] By contrast, $E^{\circ\prime}$ for the Q/H_2Q couple is pH-dependent and varies with the Nernst slope of −0.059 V/pH unit for a $2e^-/2H^+$ couple. $E^{\circ\prime}$ values for the two couples cross at pH 1.2. Below this pH, $Os(dmb)_3^{2+}$ reduction of Q is spontaneous; above this pH, $Os(dmb)_3^{3+}$ oxidation of H_2Q is spontaneous. By varying the pH, the overall reaction can be studied in either direction.

In our experiments, the kinetics of reduction of Q by $Os(dmb)_3^{2+}$ or oxidation of H_2Q by $Os(dmb)_3^{3+}$ were investigated by stopped-flow mixing with spectrophotometric monitoring at 20 °C, $I = 0.8$ M (NaCl). Stock solutions of $Os(dmb)_3^{2+}$ were freshly prepared and oxidized to Os^{III} by Cl_2,

Received: September 1, 2012
Published: November 1, 2012

   dx.doi.org/10.1021/ja308700t | J. Am. Chem. Soc. 2012, 134, 18538−18541

followed by an argon purge. All solutions were degassed with argon prior to stopped-flow mixing. *p*-Benzoquinone was purified by sublimation to give yellow crystals. The purities of Q and H_2Q were checked by ^1H NMR.

Absorption−time traces for either appearance of $Os(dmb)_3^{2+}$ by $Os(dmb)_3^{3+}$ oxidation of H_2Q, or its disappearance by oxidation by Q, were monitored at the metal-to-ligand charge transfer absorption, 480 nm. Under pseudo-first-order conditions in either Q or H_2Q, with added buffers or acids, both oxidation and reduction of Os^{II} followed first-order kinetics, with analysis of the data giving an observed rate constant k_{obs}. Typical absorption−time traces and kinetic analyses are shown in the Supporting Information, Figure SI.1.

In an initial set of experiments, $Os(dmb)_3^{2+}$ reduction of Q was investigated under pseudo-first-order conditions in [Q] with I = 0.8 M (NaCl) at T = 20 °C. In 0.16 M HCl, reduction occurred with the rate law $-d[Os^{II}]/dt = k_{obs}[Os^{II}]$ (Figure SI.2). k_{obs} varied linearly with added quinone, $[Q]_T$, with the slope k = 270 ± 4 M^{-1} s^{-1} and negligible intercept. The acid dependence of the reaction was investigated over the pH range 0.6−2.0.[11] As shown in Figure SI.3a, $k_{obs}/[Q]_T$ varied linearly with $[H^+]$, consistent with the expression $k_{obs}/[Q]_T = k_1 + k_2[H^+]$, with k_1 = 9.7 ± 2.6 M^{-1} s^{-1} and $k_2 = (2.2 \pm 0.1) \times 10^3$ M^{-2} s^{-1} (Table SI.1). The term zero-order in $[H^+]$ is consistent with outer-sphere electron transfer with $k_1 = k_{ET,Q}$,

$$Os^{II} + Q \rightarrow Os^{III} + Q^{-\bullet} \qquad k_{ET,Q} = k_1 \quad (1)$$

$$Os^{II} + Q^{-\bullet} + 2H^+ \rightarrow Os^{III} + H_2Q \qquad \text{rapid} \quad (2)$$

and the pathway first-order in $[H^+]$ is consistent with pre-protonation of Q to give HQ^+, followed by ET,

$$Q + H^+ \rightleftharpoons HQ^+ \qquad 1/K_{a,HQ^+} \quad (3)$$

$$Os^{II} + HQ^+ \rightarrow Os^{III} + HQ^{\bullet} \qquad k_{ET,HQ^+} = k_2K_{a,HQ^+} \quad (4)$$

$$Os^{II} + HQ^{\bullet} + H^+ \rightarrow Os^{III} + H_2Q \qquad \text{rapid} \quad (5)$$

With this interpretation and $pK_{a,HQ^+} = -6$, the rate constant for outer-sphere reduction of HQ^+, $k_{ET,HQ}{}^+ = (2.2 \pm 0.1) \times 10^9$ M^{-1} s^{-1}, approaches the diffusion-controlled limit in H_2O.[12] The significant rate enhancement compared to reduction of Q is not surprising since $\Delta G^{\circ\prime} = -0.07$ eV for Os^{II} reduction of HQ^+ and 0.53 eV for reduction of Q. By comparison, $HQ^{\bullet}$ disproportionation to $^1/_2Q + {}^1/_2H_2Q$ occurs with $\Delta G^{\circ\prime} = -0.7$ eV and k_{disp} = 1.1×10^9 M^{-1} s^{-1}.[8]

Reduction of Q was investigated in D_2O with added DCl with pD varied from 0.6 to 2.0.[13] Variation of $k_{obs}/[Q]_T$ with $[D^+]$ was linear (Figure SI.3b), with $k_1^D = 8.8 \pm 1.6$ M^{-1} s^{-1} and $k_2^D = (1.5 \pm 0.1) \times 10^3$ s^{-1}, yielding H_2O/D_2O solvent kinetic isotope effects (KIE; k_{H_2O}/k_{D_2O}) of 1.1 ± 0.4 for k_1 and 1.4 ± 0.1 for k_2 (Table SI.1). Although the magnitude of KIE for k_1 implies sequential ET-PT, a contribution by concerted EPT with water as the proton donor cannot be ruled out.

We also searched for a possible EPT pathway for reduction with added H_3PO_4 at fixed pH (1.3). In these experiments, the buffer ratio was held constant at $[H_3PO_4]/[H_2PO_4^-] = 4$, and $[H_3PO_4]$ was varied by increasing the total buffer concentration. Ionic strength was adjusted to 0.8 M by adding NaCl.[14] As shown in Figure SI.4a, k_{obs} increased linearly with $[H_3PO_4]$, with no sign of saturation up to $[H_3PO_4]$ = 0.48 M. From a plot of $k_{obs}/[Q]_T = k' + k_3[H_3PO_4]$, k_3 = 570 ± 20 M^{-2} s^{-1} with an intercept, $k' = k_1 + k_2[H^+]$, of 123 ± 4 M^{-1} s^{-1}. The experiment was repeated in D_2O by adding varying concentrations of D_3PO_4.[15] As shown in Figure SI.4b, $k_{obs}/[Q]_T$ increased linearly with $[D_3PO_4]$, with k_3^D = 654 ± 28 M^{-2} s^{-1} and $k_3^H/k_3^D = 0.87 \pm 0.05$.

A $[H_3PO_4]$-dependent pathway is a novel observation, consistent with pre-association of H_3PO_4 (eq 6) followed by concerted multiple-site electron−proton transfer (MS-EPT)[2a] (eq 7) with proton transfer to Q and electron transfer from Os^{II}. It is analogous to related base-catalyzed pathways in the oxidation of tyrosine, TyrOH---His + Os^{III} → $TyO^{\bullet}$ + $^+$H-His + Os^{II}.[3c,d,16] For the EPT pathway, $\Delta G^{\circ\prime} = E^{\circ\prime}(Os^{III/II}) - E^{\circ\prime}(Q^{0/-\bullet}) - 0.059(pK_{a,HQ}{}^{\bullet} - pK_{a1,H_3PO_4})$ = 0.39 eV.

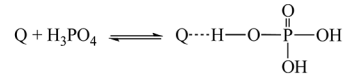

$$K_{A,Q} \quad (6)$$

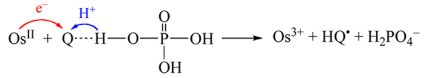

$$k_{EPT,Q\text{--}H_3PO_4} \quad (7)$$

$$Os^{II} + HQ^{\bullet} + H^+ \rightarrow Os^{III} + H_2Q \qquad \text{rapid} \quad (8)$$

The appearance of the inverse KIE for the EPT pathway was unexpected. For EPT oxidation of tyrosine by $Os(bpy)_3^{3+}$ with histidine as the proton acceptor, $k_{EPT}K_A(H_2O)/k_{EPT}K_A(D_2O)$ = 3.2.[16] As shown in eq 7, $k_3 = k_{EPT,Q\text{-}H_3PO_4}K_{A,Q}$, and the inverse isotope effect may originate in the pre-equilibrium. Small KIEs have been reported for other EPT reactions[17a] and discussed by Hammes-Schifffer and Cukier.[17b−d]

The reverse reaction, oxidation of H_2Q by $Os(dmb)_3^{3+}$, was investigated under the same conditions with H_2Q in pseudo-first-order excess from 0.2 to 4 mM over the pH range 3.5−5.6. As shown in Figures SI.1b and SI.5, under these conditions, the reaction is first-order in both Os^{III} and H_2Q, consistent with the rate law $d[Os^{II}]/dt = k_{obs}[Os^{III}]$. At pH 4.0, k_{obs} varied linearly with $[H_2Q]_T$, with $k_{obs}/[H_2Q]_T = (1.1 \pm 0.1) \times 10^4$ M^{-1} s^{-1} and a negligible intercept.

Evidence for EPT pathways was found with acetate (Ac^-) added as the acceptor base. These experiments were conducted at fixed pH (3.5) and buffer ratio $[HAc]/[Ac^-] = 10/1$, varying the concentrations of both acid and base. As shown in Figure SI.6a, $k_{obs}/[H_2Q]_T$ varies quadratically with $[Ac^-]$ over the buffer concentration range 0.05−4 M, consistent with the rate law

$$d[Os^{II}]/dt = \{k'' + k_4[Ac^-] + k_5[Ac^-]^2\}[Os^{III}][H_2Q]_T \quad (9)$$

As determined from the intercept, $k'' = (4.8 \pm 0.2) \times 10^3$ M^{-1} s^{-1}. This is consistent with the value obtained by direct measurement ($k'' = k_6 + k_7/[H^+]$, see below). As shown in Figure SI.6a, the rate constants k_4 and k_5 were obtained by fitting the extended data set to give $k_4 = (2.6 \pm 0.1) \times 10^5$ M^{-2} s^{-1} and k_5 = $(8.2 \pm 0.1) \times 10^5$ M^{-3} s^{-1}.

The experiments with added HAc/Ac^- were repeated in D_2O at pD 4.1 with the same rate law behavior (Figure SI.6b). Analysis of the results gave $k''(D_2O) = (1.8 \pm 0.1) \times 10^3$ M^{-1} s^{-1}, consistent with the value obtained in D_2O with no added Ac^- (see below), with $k_4^D = (9.9 \pm 0.3) \times 10^4$ M^{-2} s^{-1} and $k_5^D = (2.9 \pm 0.2) \times 10^5$ M^{-3} s^{-1}. Based on these results and those obtained in H_2O, the H_2O/D_2O KIE values are 2.6 ± 0.1 for k_4 and 2.8 ± 0.2 for k_5.

The most straightforward interpretation of the term first-order in Ac^- is that, as found for tyrosine oxidation by $Os(bpy)_3^{3+}$, pre-association occurs between Ac^- and H_2Q, followed by MS-EPT:

dx.doi.org/10.1021/ja308700t | J. Am. Chem. Soc. 2012, 134, 18538−18541

$$H_2Q + Ac^- \rightleftharpoons Ac^-\text{---}H_2Q \qquad K_A \quad (10)$$

$$Os^{III} + Ac^-\text{---}H_2Q \rightarrow Os^{II} + HQ^\bullet + HAc \qquad k_{EPT} \quad (11)$$

$$Os^{III} + HQ^\bullet \rightarrow Os^{II} + Q + H^+ \qquad \text{rapid} \quad (12)$$

Given the similarity in KIE values and the high concentrations of Ac^- used, the squared term in $[Ac^-]$ may arise from a parallel mechanism, but with ion-pairing with the tri-cationic metal complex oxidant by a second Ac^-, followed by MS-EPT oxidation of H_2Q---Ac^- (eqs 13 and 14):

$$H_2Q + Ac^- \rightleftharpoons Ac^-\text{---}H_2Q \qquad K_A \quad (10)$$

$$(Os^{III})^{3+} + Ac^- \rightarrow (Os^{III})^{3+}, Ac^- \qquad K_{IP} \quad (13)$$

$$(Os^{III})^{3+}, Ac^- + Ac^-\text{---}H_2Q \rightarrow (Os^{II})^{2+} + HQ^\bullet + HAc + Ac^- \qquad k'_{EPT} \quad (14)$$

$$Os^{III} + HQ^\bullet \rightarrow Os^{II} + Q + H^+ \qquad \text{rapid} \quad (12)$$

Other interpretations are possible, including formation of a doubly H-bonded Ac^- adduct with H_2Q.

With this interpretation, $k_4 = K_A k_{EPT}$ and $k_5 = K_{IP} K_A k'_{EPT}$, with K_A the association constant between Ac^- and H_2Q and K_{IP} the ion pair constant between $Os(dmb)_3^{3+}$ and Ac^-. The observed KIEs include contributions from the pre-equilibria but are presumably dominated by the KIEs for the EPT steps.[3b−d]

An additional pH-dependent term appears in the rate law from oxidation of HQ^-. This term was investigated by stopped-flow measurements over the pH range 3.5−5.6 with added 0.05 M Ac^- buffer at I = 0.8 M. Under these conditions, there are contributions to k_{obs} from the pathways first- and second-order in $[Ac^-]$ (eq 9). A correction was made to k_{obs} for their contributions by using the known values for k_4 and k_5 with $[Ac^-] = K_{a,HAc}[buffer]/([H^+] + K_{a,HAc})$. As shown in Figure SI.7a, under these conditions $k_{obs}/[H_2Q]_T$ varied linearly with $[H^+]$ with $k_6 = (3.5 \pm 0.1) \times 10^3\ M^{-1}\ s^{-1}$ and $k_7 = 0.54 \pm 0.01\ s^{-1}$:

$$\frac{k_{obs}}{[H_2Q]_T} = k_4[Ac^-] + k_5[Ac^-]^2 + k_6 + \frac{k_7}{[H^+]} \qquad (15)$$

The pD dependence was also investigated for this pathway in D_2O solutions dilute in added Ac^- (0.01 M) free of contributions from the MS-EPT pathways. A fit of a plot of $k_{obs}/[H_2Q]$ vs pD (Figure SI.7b) to the expression $k_{obs}/[H_2Q]_T = k_6^D + k_7^D/[D^+]$ gave $k_6^D = (1.0 \pm 0.1) \times 10^3\ M^{-1}\ s^{-1}$ and $k_7^D = (9.8 \pm 0.2) \times 10^{-2}\ s^{-1}$. As noted above, $k''^D = k_6^D + k_7^D/[D^+]$.[13] Based on these values, H_2O/D_2O KIEs were 3.5 ± 0.2 for k_6 and 5.5 ± 0.1 for k_7.

For the pathway through k_7, the appearance of the inverse first-order dependence in $[H^+]$ is consistent with deprotonation of H_2Q to give HQ^-, followed by ET:

$$H_2Q \rightleftharpoons HQ^- + H^+ \qquad K_{a1,H_2Q} \quad (16)$$

$$Os^{III}HQ^- \rightarrow Os^{II} + HQ^\bullet \qquad k_{ET,HQ^-} = k_7/K_{a1,H_2Q} \quad (17)$$

$$Os^{III}HQ^\bullet \rightarrow Os^{II} + Q + H^+ \qquad \text{rapid} \quad (18)$$

With $pK_{a1,H_2Q} = 9.82$[18] and $k_7 = 0.54 \pm 0.01\ s^{-1}$, $k_{ET,HQ^-} = (3.6 \pm 0.1) \times 10^9\ M^{-1}\ s^{-1}$ was obtained, near the diffusion-controlled limit of $7 \times 10^9\ M^{-1}\ s^{-1}$.[19] Given $pK_{a1,D_2Q} \approx 10.4$ in D_2O,[20] $K_{a1,H_2Q}(H_2O)/K_{a,1,D_2Q}(D_2O) \approx 4.0$, and the KIE for k_{ET,HQ^-} is ~1.4, consistent with outer-sphere oxidation as in eq 17.

The rate law and KIE for the k_6 term are consistent with electron-transfer oxidation of H_2Q but with simultaneous proton transfer to the solvent (eq 19):

$$Os^{III} + H_2O\text{---}H_2Q \rightarrow Os^{II} + HQ^\bullet + H_3O \qquad k_{EPT,H_2Q} = k_6 \quad (19)$$

$$Os^{III} + HQ^\bullet \rightarrow Os^{II} + Q + H^+ \qquad \text{rapid} \quad (20)$$

This pathway is kinetically indistinguishable from outer-sphere oxidation of H_2Q to $H_2Q^{\bullet+}$ followed by proton equilibration from $H_2Q^{\bullet+}$ with $K_{a,H2Q}^{\bullet+} = 10$ (eqs 21 and 22):

$$Os^{III} + H_2Q \rightarrow Os^{II} + H_2O^{\bullet+} \qquad k_{ET,H_2Q} = k_6 \quad (21)$$

$$H_2Q^{\bullet+} \rightarrow HQ^\bullet + H^+ \qquad K_{a,H_2Q^{\bullet+}} \quad (22)$$

$$HQ^\bullet \rightarrow {}^1/_2\,H_2Q + {}^1/_2\,Q \qquad \text{rapid} \quad (23)$$

However, the magnitude of the KIE points to a dominant role for MS-EPT with the solvent as the proton acceptor. Once again, EPT is energetically favored. For the initial ET step in eq 21, $\Delta G^{\circ\prime} = +0.47$ eV based on $E^{\circ\prime}$ values for the two couples. For the MS-EPT step (eq 19), $\Delta G^{\circ\prime} = -[E^{\circ\prime}(Os^{III/II}) - E^{\circ\prime}(H_2Q^{\bullet+}/H_2Q)] - 0.059(pK_a(H_3O^+) - pK_a(H_2Q^{\bullet+}) = 0.41$ eV.[21]

This result highlights an important role for an EPT pathway in the oxidation of H_2Q in water, in this case with a solvent molecule or water cluster acting as the proton acceptor as reported earlier for phenol oxidation by Stanbury[22a] and Saveant.[22b] By comparison, oxidation of H_2Q by the Ru^{III} oxidant, $Ru^{III}(bpy)_2(py)(OH)^{2+}$, occurs by direct EPT with both electron and proton transfer to the Ru^{III}−OH^{2+} acceptor,

$$Ru^{III}OH^{2+} + H_2Q \rightleftharpoons Ru^{III}OH^{2+}\text{---}H_2Q \quad (24)$$

$$Ru^{III}OH^{2+}\text{---}H_2Q \rightarrow Ru^{II}OH_2{}^{2+} + HQ^\bullet \quad (25)$$

$$Ru^{III}OH^{2+} + HQ^\bullet \rightarrow Ru^{II}OH_2{}^{2+} + Q \qquad \text{rapid} \quad (26)$$

This reaction occurs with a KIE of 9.7 ± 0.1.[5c]

Our results highlight a remarkable versatility in the redox interconversion between quinone and hydroquinone by the outer-sphere $Os(dmb)_3^{3+/2+}$ couple. This versatility arises from the nature of the reagents themselves with accessibility to $1e^-$ intermediates $Q^{-\bullet}$ and $H_2Q^{\bullet+}$ by $1e^-$ reduction of Q or oxidation of H_2Q, or to $HQ^\bullet$ and by their use of EPT pathways with concerted e^-/H^+ transfer to Q or from H_2Q. A summary is given in Scheme 1 for the reduction of Q and in Scheme 2 for the oxidation of H_2Q.

Important insights also emerge for the individual pathways:

(i) Specific acid and base catalysis occur for both reduction of Q and oxidation of H_2Q. This is due to the relatively high energy of the $1e^-$ intermediates $Q^{-\bullet}$ and $H_2Q^{\bullet+}$, which favors pathways involving PT-ET or ET-PT with prior formation of HQ^+ or HQ^-.

Scheme 1

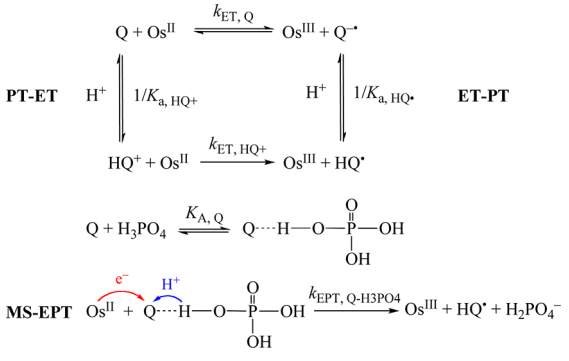

dx.doi.org/10.1021/ja308700t | J. Am. Chem. Soc. 2012, 134, 18538−18541

Scheme 2

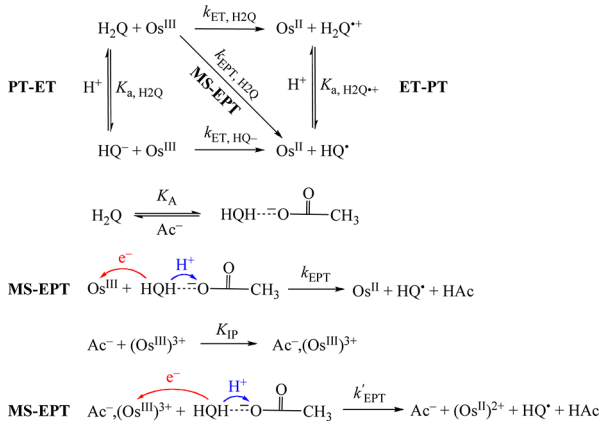

(ii) General acid and base catalysis appears with the acid (H_3PO_4) or base (Ac^-) forms of added buffers due to the intervention of concerted EPT pathways which give $HQ^\bullet$ directly by reduction of Q---HA or oxidation of Q---H_2Q. This is, no doubt, a general phenomenon and, as for tyrosine, will appear generally with added proton acceptor bases including use of these couples in biology.

(iii) In the oxidation of H_2Q by Os^{III}, the dominant mechanism is EPT with concerted proton transfer to the solvent.

■ ASSOCIATED CONTENT

Ⓢ Supporting Information

Experimental details and analyses. This material is available free of charge via the Internet at http://pubs.acs.org.

■ AUTHOR INFORMATION

Corresponding Author

tjmeyer@email.unc.edu

Notes

The authors declare no competing financial interest.

■ ACKNOWLEDGMENTS

This work has been supported by the National Science Foundation under grant CHE-0957215, supporting M.-T.Z. (T.J.M.) and C.J.G. (T.J.M. and H.T.). N.S. (T.J.M.) is supported through the Richard T. and Hugh G. Chatham Fund for Faculty Research and Development. R.A.B. (T.J.M.) is supported as part of the UNC EFRC: Center for Solar Fuels, an Energy Frontier Research Center funded by the U.S. Department of Energy, Office of Science, Office of Basic Energy Sciences, under Award No. DE-SC0001011. We thank Dr. Zhen Fang (UNC EFRC) for synthesis of the Os(II) complex.

■ REFERENCES

(1) (a) Müh, F.; Glöckner, C.; Hellmich, J.; Zouni, A. *BBA-Bioenergetics* **2012**, *1817*, 44. (b) Nohl, H.; Jordan, W.; Youngman, R. J. *Adv. Free Radical Biol.* **1986**, *2*, 211. (c) Efremov, R. G.; Baradaran, R.; Sazanov, L. A. *Nature* **2010**, *465*, 441.

(2) (a) Weinberg, D. R.; Gagliardi, C. J.; Hull, J. F.; Murphy, C. F.; Kent, C. A.; Westlake, B. C.; Paul, A.; Ess, D. H.; McCafferty, D. G.; Meyer, T. J. *Chem. Rev.* **2012**, *112*, 4016. (b) Huynh, M. H. V.; Meyer, T. J. *Chem. Rev.* **2007**, *107*, 5004. (c) Meyer, T. J.; Huynh, M. H. V.; Thorp, H. H. *Angew. Chem., Int. Ed.* **2007**, *46*, 5284. (d) Stubbe, J.; van der Donk, W. A. *Chem. Rev.* **1998**, *98*, 705. (e) Reece, S. Y.; Hodgkiss, J. M.; Stubbe, J.; Nocera, D. G. *Philos. Trans. R. Soc. B* **2006**, *361*, 1351.

(3) (a) Zhang, M. T.; Irebo, T.; Johansson, O.; Hammarström, L. *J. Am. Chem. Soc.* **2011**, *133*, 13224. (b) Gagliardi, C. J.; Jurss, J. W.; Thorp, H. H.; Meyer, T. J. *Inorg. Chem.* **2011**, *50*, 2076. (c) Fecenko, C. J.; Thorp, H. H.; Meyer, T. J. *J. Am. Chem. Soc.* **2007**, *129*, 15098. (d) Fecenko, C. J.; Meyer, T. J.; Thorp, H. H. *J. Am. Chem. Soc.* **2006**, *128*, 11020. (e) Sjödin, M.; Styring, S.; Åkermark, B.; Sun, L. C.; Hammarström, L. *J. Am. Chem. Soc.* **2000**, *122*, 3932.

(4) Ekberg, M.; Pötsch, S.; Sandin, E.; Thunnissen, M.; Nordlund, P.; Sahlin, M.; Sjöberg, B. M. *J. Biol. Chem.* **1998**, *273*, 21003.

(5) (a) Waidmann, C. R.; Zhou, X.; Tsai, E. A.; Kaminsky, W.; Hrovat, D. A.; Borden, W. T.; Mayer, J. M. *J. Am. Chem. Soc.* **2009**, *131*, 4729. (b) Lam, W. W. Y.; Lee, M. F. W.; Lau, T. C. *Inorg. Chem.* **2006**, *45*, 315. (c) Binstead, R. A.; McGuire, M. E.; Dovletoglou, A.; Seok, W. K.; Roecker, L. E.; Meyer, T. J. *J. Am. Chem. Soc.* **1992**, *114*, 173. (d) Kawashima, T.; Ohkubo, K.; Fukuzumi, S. *Phys. Chem. Chem. Phys.* **2011**, *13*, 3344. (e) Clemmer, J. D.; Hogaboom, G. K.; Holwerda, R. A. *Inorg. Chem.* **1979**, *18*, 2567.

(6) (a) Sasaki, K.; Kashimura, T.; Ohura, M.; Ohsaki, Y.; Ohta, N. *J. Electrochem. Soc.* **1990**, *137*, 2437. (b) Lehmann, M. W.; Evans, D. H. *J. Electroanal. Chem.* **2001**, *500*, 12. (c) Astudillo, P. D.; Tiburcio, J.; González, F. J. *J. Electroanal. Chem.* **2007**, *604*, 57. (d) Gupta, N.; Linschitz, H. *J. Am. Chem. Soc.* **1997**, *119*, 6384.

(7) Laviron, E. *J. Electroanal. Chem.* **1984**, *169*, 29.

(8) Adams, G. E.; Michael, B. D. *Trans. Faraday Soc.* **1967**, *63*, 1171.

(9) Warren, J. J.; Tronic, T. A.; Mayer, J. M. *Chem. Rev.* **2010**, *110*, 6961.

(10) (a) Chan, M. S.; Wahl, A. C. *J. Phys. Chem.* **1978**, *82*, 2542. (b) Song, N.; Stanbury, D. M. *Inorg. Chem.* **2012**, *51*, 4909.

(11) pH = $-\log [H^+] - \log \gamma_{H^+}$. In this expression, γ_{H^+} is the activity coefficient of the proton at I = 0.8 M.

(12) (a) Alberty, R. A.; Hammes, G. G. *J. Phys. Chem.* **1958**, *62*, 154. (b) Hammes, G. G.; Amdur, I. *Principles of chemical kinetics*; Academic Press: New York, 1978. (c) Espenson, J. H. *Chemical kinetics and reaction mechanisms*; McGraw-Hill: New York, 1995.

(13) pD = $-\log [D^+] - \log \gamma_{D^+}$, assuming that $\gamma_{D^+} = \gamma_{H^+}$.

(14) $pK_{a1,H_3PO_4} = -1.79$ at I = 0.8 M was converted from the reported values, 2.127 at zero ionic strength; see SI.

(15) pK_{a1,D_3PO_4} = 2.06 at I = 0.8 M in D_2O was converted from the reported values, 2.3981 at zero ionic strength with $\gamma_{H^+} = \gamma_{D^+}$. pD = pH meter reading + 0.4; see SI.

(16) Murphy, C. F. Ph.D. Dissertation, University of North Carolina at Chapel Hill, 2009.

(17) (a) Biczók, L.; Gupta, N.; Linschitz, H. *J. Am. Chem. Soc.* **1997**, *119*, 12601. (b) Edwards, S. J.; Soudackov, A. V.; Hammes-Schiffer, S. *J. Phys. Chem. A* **2009**, *113*, 2117. (c) Cukier, R. I. *J. Phys. Chem.* **1994**, *98*, 2377. (d) Hazra, A.; Soudackov, A. V.; Hammes-Schiffer, S. *J. Phys. Chem. Lett.* **2011**, *2*, 36.

(18) pK_{a1,H_2Q} = 9.82 in H_2O at I = 0.8 M was corrected from 9.85 at I = 0.65 M; see SI.

(19) The bimolecular diffusion control limit, $k_D = 3 \times 10^9\ M^{-1}\ s^{-1}$, was corrected for the electrostatic interaction between $(Os^{III})^{3+}$ and HQ^-; see SI.

(20) Martin, R. B. *Science* **1963**, *139*, 1198.

(21) Under standard conditons, theoretical thermodynamic calculation requires $[H_2O]$ = 1 M, which gives $pK_a(H_3O^+) = 0$.

(22) (a) Song, N.; Stanbury, D. M. *Inorg. Chem.* **2008**, *47*, 11458. (b) Bonin, J.; Costentin, C.; Louault, C.; Robert, M.; Routier, M.; Savéant, J. M. *Proc. Natl. Acad. Sci. U.S.A.* **2010**, *107*, 3367.